

Parallelization of a treecode

Riccardo Valdarnini¹

SISSA – International School for Advanced Studies, Via Beirut 2/4, Trieste, Italy

Abstract

I describe here the performance of a parallel treecode with individual particle timesteps. The code is based on the Barnes-Hut algorithm and runs cosmological N-body simulations on parallel machines with a distributed memory architecture using the MPI message-passing library. For a configuration with a constant number of particles per processor the scalability of the code was tested up to $P = 128$ processors on an IBM SP4 machine. In the large P limit the average CPU time per processor necessary for solving the gravitational interactions is $\sim 10\%$ higher than that expected from the ideal scaling relation. The processor domains are determined every large timestep according to a recursive orthogonal bisection, using a weighting scheme which takes into account the total particle computational load within the timestep. The results of the numerical tests show that the load balancing efficiency L of the code is high ($\gtrsim 90\%$) up to $P = 32$, and decreases to $L \sim 80\%$ when $P = 128$. In the latter case it is found that some aspects of the code performance are affected by machine hardware, while the proposed weighting scheme can achieve a load balance as high as $L \sim 90\%$ even in the large P limit.

Key words: Methods : numerical – Cosmology : simulations

PACS: 02.60; 95.75 Pq; 98.80

1 Introduction

According to the standard picture the observed structure in the universe has arisen via gravitational instability from the time evolution of initial irregularities in the matter density distribution. These perturbations grew under their own gravity and during early epochs their cosmic evolution can be described according to standard linear perturbation theory. At late epochs the evolution of structure on scales of relevant cosmological interest is characterized by nonlinearity. Numerical simulations play a fundamental role in improving

¹ E-mail: valda@sissa.it

the theoretical understanding of structure formation. This approach has received a large impulse from the huge growth of computer technology in the last two decades. Cosmological N-body simulations are now widely used as a fundamental tool in modern cosmology for testing viable theories of structure formation. The most important task of cosmological codes is the computation of the gravitational forces of the system. Several methods have been developed to solve the large-scale gravitational field (see, e.g., Bertschinger 1998 for a review). A popular approach is the tree algorithm (Appel 1985, Hernquist 1987). The particle distribution of the system is arranged into a hierarchy of cubes and the force on an individual particle is computed by a summation of the multipole expansion of the cubes. The main advantage of a tree-based code is the computational cost of a force evaluation, which scales with the particle number N_p as $\propto N_p \log N_p$. This makes tree codes particularly indicated in simulations where a large number of particles is required. Another important point in favour of tree codes is that individual timesteps for all of the particles can be implemented easily, which allows a substantial speed-up of the force evaluation for a clustered distribution. For a typical evolved distribution the particles located in high-density regions will need to be advanced using the smallest timesteps, but they represent only a small fraction of the total particle number. If the particles are advanced with a single timestep Δt , the overall accuracy in the orbit integration is then maintained only if Δt is the minimum timestep Δt_{min} of the particle configuration. In the single-step integration scheme the force of all the particles is re-evaluated at each step, but if Δt_{min} becomes very small this implies that a large amount of computational work is wasted in calculating the force of particles in regions where the imposed global accuracy is not required. If individual timesteps are allowed, the accelerations are then evaluated at each step only for those particles which have been identified according to a specified stability criterion.

An important task is the improvement of the dynamic range of the simulations. Large simulation volumes are required for statistical purposes but, at the same time, modeling the formation and evolution of each individual galaxy in the simulated volume requires that a realistic simulation should be implemented with $10^8 \sim 10^9$ particles. This computational task can be efficiently solved if the code is adapted to work on a parallel machine where many processors are linked together with a communication network. If the architecture of the machine is memory-distributed the optimal code should distribute the computational load in an even way on all the processors and, at the same time, minimize the communications among all the processors. Because of the long-range nature of gravity the latter task is inherently difficult. On the other hand, with respect to a serial code for a network of P processors the computation reward in terms of CPU time is expected to be close to $\sim P$. These arguments have led a number of authors to parallelize treecodes (Salmon 1991, Warren 1994, Dubinski 1996, Davé, Dubinski & Hernquist 1997, Lia & Carraro 2000, Springel, Yoshida & White 2001, Miocchi

& Capuzzo-Dolcetta 2002). In this paper I present a parallel implementation of a multistep treecode based on the Barnes-Hut (1986, BH) algorithm. The code is cosmological and uses the MPI message library. The paper is organized as follows. In sect. 2 the tree algorithm is presented and the dependence of the acceleration errors on the tree-opening parameter θ is discussed, together with the implemented scheme for the parallelization of the treecode. Parallel performances are discussed in sect. 3 and the main results are summarized in sect. 4.

2 Parallelization of a treecode

The BH algorithm works by subdividing a root box of size L , which contains all of the simulation particles, into 8 subvolumes of size $L/2$. This procedure is then repeated for each of the subcubes and continues until the remaining cells or nodes are empty or have one particle. After the k -th iteration the size of the subcubes is $l_k = L/2^k$. After the tree construction is complete the multipole moments of the mass distribution inside the cells are computed starting from the smallest cells and proceeding up to the root cell. The moments of the cells are typically approximated up to quadrupole order. For each particle the acceleration is evaluated by summing the contribution of all of the cells and particles which are in an interaction list. The list is constructed starting from the root cell and descending the tree down to a required level of accuracy. At each level a cell of the tree is accepted if it satisfies an accuracy criterion. If the cell fails this criterion then it is opened, the particles contained are added to the interaction list and the accuracy criterion is applied again for the remaining subcells. BH have introduced the following acceptance criterion for the examined cell

$$d > l_k/\theta, \tag{1}$$

where d is the distance between the center of mass (c.o.m.) of the cell and the particle position, θ is an input parameter which controls the accuracy of the force evaluation. When θ gets smaller more cells are added to the interaction lists and this implies a more accurate force evaluation. For $\theta \rightarrow 0$ one recovers the direct summation. When θ is large ($\simeq 1$) and the c.o.m. is close to the edge of the cell an acceptance criterion which avoids possible errors in the force calculation is given by (Barnes 1994, Dubinski 1996)

$$d > l_k/\theta + \delta, \tag{2}$$

where δ is the distance between the cell c.o.m. and its geometrical center.

2.1 Domain decomposition

The spatial domains of the processors are determined according to the orthogonal recursion bisection (ORB, Salmon 1991). The computational volume is first cut along the x-axis at a position x_c such that

$$\sum_{i<} w_i \simeq \sum_{i>} w_i, \tag{3}$$

where the summations are over all of the particles with $x_i < x_c$ or $x_i > x_c$ and $w_i \propto N_{OP}(i)$ is a weight assigned to each particle proportional to the number of floating point operations (i.e. the computational work) which are necessary to compute the particle force.

When the root x_c has been determined the particles are then exchanged between the processors until all of the particles with $x_i < x_c$ belong to the first $P/2$ processors, and those with $x_i > x_c$ are in the second $P/2$ processors. The whole procedure is repeated recursively, cycling through the cartesian dimensions, until the total number of subdivisions of the computational volume is $\log_2 P$ (with this algorithm P is constrained to be a power of two). At the end of the domain decomposition, the subvolumes will enclose a subset of particles with approximately an equal amount of computational work. The calculation of the forces is then approximately load-balanced among all of the processors.

The parallel treecode presented here uses individual particle timesteps and the number of active particles N_{act} for which it is necessary to calculate the forces is highly variable with the current timestep. This number at a given time can be a small fraction of the total particle number. In such cases the load balancing scheme, which has been determined according to the ORB algorithm at the previous step, can be significantly degraded. One solution is to perform the ORB at each timestep, but this implies a communication overhead when N_{act} is small. In the multistep integration scheme Δt_0 is the maximum allowed particle timestep and the particle positions are synchronized when the simulation time t is a multiple of Δt_0 ; see, e.g., Hernquist & Katz (1989) for more details. In the parallel treecode presented here, the ORB domain decomposition is applied every large timestep Δt_0 , when the simulation time t is $n\Delta t_0$. The load-balancing of the code is presented in sect. 3.2., where it is discussed how the performances are dependent on the computational weight w_i assigned to each particle.

2.2 Construction of the local essential tree

A BH tree is constructed by each processor using the particles located in the processor subvolume. However, the local tree does not contain all of the information needed to perform the force calculation for the processor particles. For these particles a subset of cells must be imported from the trees of the other processors according to the opening angle criterion applied to the remote cells. Each processor then receives a set of partial trees which are merged with the local tree to construct a local essential tree (Dubinski 1996). The new local tree contains all of the information with which the forces of the local particles can be consistently calculated.

The communications between processors of nodes from different trees imply that in order to graft the imported cells onto the processor local trees it is necessary to adopt an efficient addressing scheme for the memory location of the nodes. This is easily obtained if the construction of the local trees starts from a root box of size L , common to all of the processors. Because of the ORB the spatial domains of the particle processors will occupy a fraction $\sim 1/P$ of the computational volume L^3 . This implies in the tree construction a small memory overhead. The main advantage is however that now the non-empty cells of the local trees have the same position and size in all of the processors. Each cell is then uniquely identified by a set of integers $\{j_1, j_2, \dots\}$, with each integer ranging from 0 to 7 which identifies one of the 8 subcells of the parent cell. These integers can be conveniently mapped onto a single integer word of maximum bit length $3k_{max}$, where k_{max} is the maximum subdivision level of the tree. For a 64 bit key $k_{max} \leq 21$. This integer word represents the binary key of the cell. When a cell of the tree is requested by a remote processor to construct its local tree, the associated key is sent together with the mass, c.o.m. and multipole moments of the cell. The receiving processor then uses this key to quickly identify the cell location in the local tree and to add the new cell to the local tree. A similar addressing scheme has been implemented, in their version of a parallel treecode, also by Mocchi & Capuzzo-Dolcetta (2002).

The construction of the local essential trees is the most complicated part to be implemented in a parallel treecode. A simple translation of the logic of the BH opening criterion to a parallel treecode on a distributed memory machine implies that each particle of each processor should apply the opening criterion to the tree nodes of the remaining $P - 1$ processors. This approach is clearly impractical because of the large communication cost needed to exchange particle positions or tree nodes between processors. An efficient construction of the local essential tree is obtained instead as follows (Valdarnini 2002a). This construction method is similar, with slight modifications, to the one described by Dubinski (1996).

Table 1
Cosmological parameters of the simulations

model	Ω_m	h	a_{fin}	$L(h^{-1}Mpc)$	σ_8
Λ CDM	0.3	0.7	11	200	1.1
CDM	1	0.5	40	11.11	0.6

i) Once the ORB has been completed and each processor has received the particle subset with spatial coordinates within its spatial domains, the local trees are constructed according to BH in each of the processors P_k , where k is a processor index ranging from 0 to $P - 1$.

ii a) In a first version the local essential trees were constructed as in Dubinski (1996). A list of the cells of the processor's local tree is created, with the criterion that they must contain a number of particles $\lesssim N_c (\sim 32)$. This grouping scheme was introduced by Barnes (1990), in order to significantly reduce the number of particle-cell applications of the opening criterion necessary for constructing the interaction lists of the particles. The opening angle criterion (1) or (2) is applied between one of the grouped cells and the examined cells: d is now the minimum distance between the cells c.o.m. and the grouped cell. The obtained interaction list of cells by definition satisfies Eq. 1 or 2 for all the particles within the grouped cell.

This interaction list can then be used in the force calculation of all these particles. The speed-up depends on the distribution of the clustered particles and on machine hardware, Barnes (1990) suggests it can be a factor of 3 to 5. However N_c cannot be too large, otherwise for a given grouped cell the generated interaction lists will contain a number of cells largely in excess of those effectively needed. As a compromise, it is found $N_c \lesssim 64$ (Barnes 1990). For a multistep treecode the application of the grouping method for reducing the cost of the list construction is not straightforward. This is because the number of active particles N_{act} at a given time can be a small fraction of the total particle number. In such cases, the advantages of having a unique interaction list for a small particle subset can be outweighed by the computational cost necessary for constructing it. The parallel treecode described here uses individual particle timesteps and this grouping method has not been implemented to construct the cell interaction lists of the particle forces.

After the list of grouped cells has been created, each processor imports the root nodes necessary for the construction of the local essential tree from the other processors. These nodes are found by applying in the exporting processor the opening angle criterion to its local tree. The list of cells and particles obtained is sent to the importing processor, where it is merged with the local tree at the corresponding nodes. These nodes are identified using the binary keys of the imported nodes. At the end of these steps each processor has the tree structure necessary to compute the forces of the local particle distribution.

ii b) The communications between processors can be significantly reduced if one adopts the following criterion to construct the partial trees which will be exchanged between processors. After the local trees have been constructed, each processor applies the opening angle criterion between the nodes of its local tree and the closest point of the volume of another processor P_k . The partial tree obtained contains by definition all of the nodes of the local processor necessary to evaluate the forces of the particles located in the processor P_k . This procedure is performed at the same time by each processor for all of the remaining $P - 1$ processors. At the end, each processor has $P - 1$ lists of nodes which are necessary for the construction of the local essential trees in the other processors. The processor boundaries are determined during the ORB and are communicated between all of the processors after its completion. Hence, the main advantage of this procedure is that all of the communications between processors necessary for the construction of the local essential trees are performed in a single all-to-all message-passing routine. The drawback of this scheme is the memory overhead, because each processor imports from another processor a list of nodes in excess of those effectively needed to perform the force calculation, and also in excess of those which would have been imported with the previous procedure. As a rule of thumb, it has been found that for $\theta = 0.4$ a processor with N_p particles and N_c cells imports $\sim N_p/8 - N_p/4$ particles and $\sim N_c$ cells. The number of imported nodes is independent of the processor number. The value $\theta = 0.4$ is a lower limit that guarantees reasonable accuracy in the force evaluation in many simulations. In the communication phase between processors, mass and position are imported for each particle, and the mass, c.o.m., quadrupole moment and the binary key are imported for each cell. The memory required by a single processor to construct the local essential tree is then approximately a factor ~ 2 larger than that used in the implementation of the local tree. This memory requirement can be efficiently managed using dynamic allocation, and is not significantly larger than that required by other schemes used to construct the local essential tree (e.g., Dubinski 1996).

2.3 Force calculation

After the construction of the local essential trees has been completed, each processor proceeds asynchronously to calculate the forces of the active particles in its computational volume up to the quadrupole order. The code has incorporated periodic boundary conditions and comoving coordinates. Hence the forces obtained from the interaction lists of the local essential trees must be corrected to take into account the contribution of the images. (Davé, Dubinski & Hernquist 1997, Springel, Yoshida & White 2001). These correction terms are calculated before the simulation using the Ewald method (Hernquist, Bouchet & Suto 1991). The corrections are computed on a cubic mesh of size

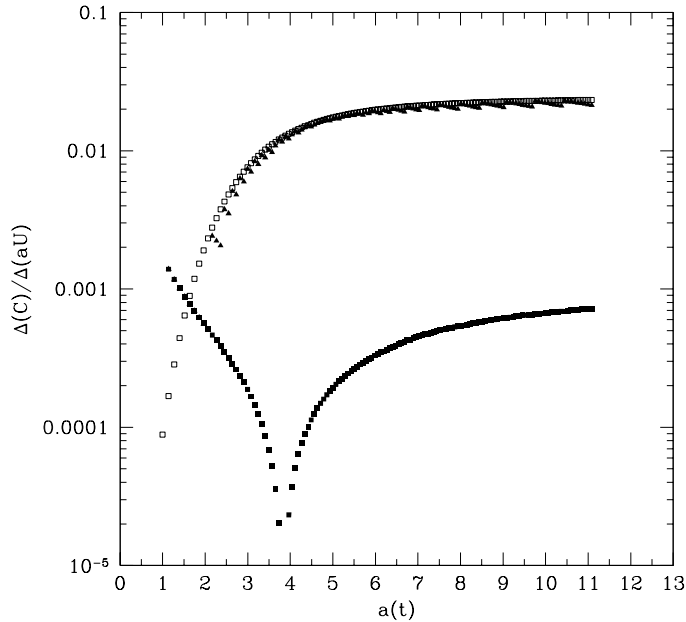


Fig. 1. The relative error $\Delta C/\Delta aU$ in the cosmic energy equation is shown as a function of the expansion factor $a(t)$ for different simulations. The chosen cosmological model is a flat CDM with a cosmological constant, $\Omega_m = 0.3$ and $h = 0.7$. The simulations are performed in a $200h^{-1}Mpc$ comoving box with 84^3 particles. Filled squares refer to a simulation (S1L) with forces calculated using $\theta = 0.4$ and quadrupole moments. Filled triangles correspond to a run (S2L) with the same simulation parameters but with $\theta = \theta(t)$ which is controlled by Eq. 5 (open square). Values of $\Delta C/\Delta aU$ for the corresponding parallel runs are not displayed because they overlap with the plotted symbols.

L with 50^3 grid points and are stored in a file. During the force computation, a linear interpolation is used to calculate the correction terms corresponding to the particle positions from the stored values.

In a cosmological simulation, the evaluation of the peculiar forces in the linear regime is subject to large relative errors. This is because for a nearly homogeneous distribution, the net force acting on a particle is the result of the cancellation of the large partial forces determined from the whole mass distribution. From a set of test simulations Davé, Dubinski & Hernquist (1997) found that in the linear regime, when $\theta = 0.4$ and the cell moments are evaluated up to the quadrupole order, the relative errors in the forces are $\lesssim 7\%$. This problem is not present at late epochs, when the clustering of the simulation particles is highly evolved and even for $\theta \simeq 1$ the relative errors in the forces are small ($\lesssim 2\%$). This imposes in the simulation the necessity of varying θ according to the clustering evolution, since the computational cost

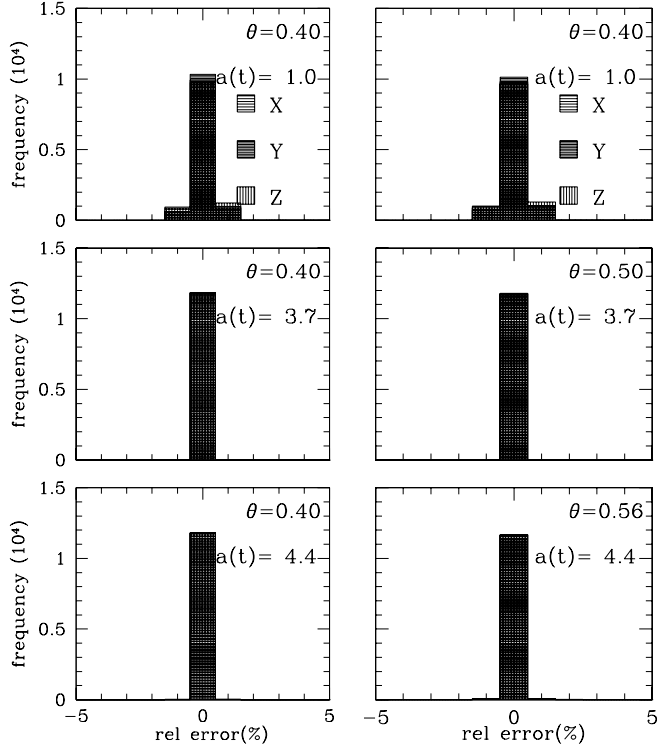


Fig. 2. For two simulations with different values of θ the distribution of the relative errors in the force components is shown for several values of $a(t)$. The simulations are those of Fig. 1. Left column is for the run S1L with $\theta = 0.4$ and right column is for the run S2L with $\theta = \theta(t)$.

of evaluating the forces with a small value of θ is wasted in the non-linear regime. In this regime, the forces can be evaluated with an accuracy as good as that obtained in the linear regime, though using a higher value of θ .

After several tests it was found that a good criterion to control the value of $\theta(t)$ is that at any given simulation time t the energy conservation must be satisfied with a specified level of accuracy. The Lyzer-Irvine equation is

$$a^4 T + aU - \int U da = C, \quad (4)$$

where $a = a(t)$ is the expansion factor, T is the kinetic energy of the system, U is the potential energy and C is a constant. The accuracy of the integration can be measured by the quantity $err(t) = |\Delta(C)/\Delta(aU)|$, where Δf denotes the change of f with respect to its initial value. Fig. 1 shows the time evolution of $err(t)$ versus the expansion factor for different test simulations. The cosmological model considered is a flat CDM model, with a vacuum energy density $\Omega_\Lambda = 0.7$, matter density parameter $\Omega_m = 0.3$ and Hubble constant $h = 0.7$

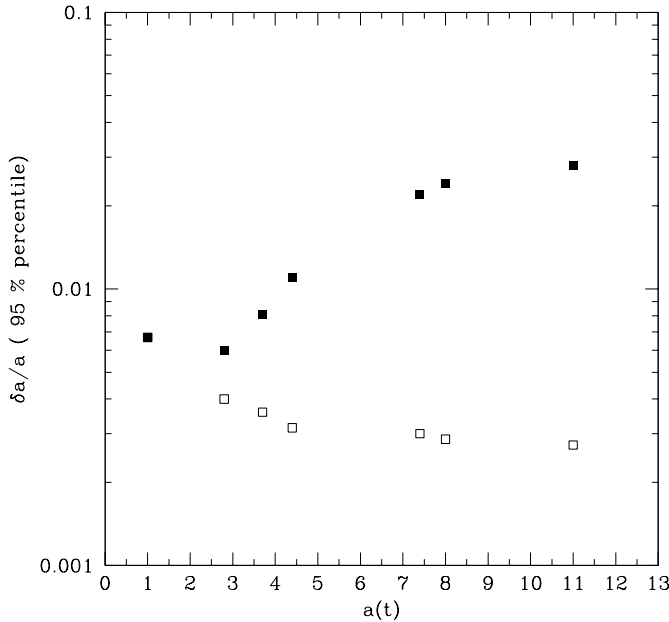


Fig. 3. Time evolution of the relative error $\delta a/a$ at the 95% percentile of the cumulative distribution for simulations S1L (open squares) and S2L (filled squares). The relative error is defined as $\delta a/a \equiv |a - a_D|/|a_D|$, where a_D is the particle acceleration evaluated in the direct summation limit.

in units of $100 K m sec^{-1} Mpc^{-1}$. Table 1 presents the main parameters of the model. The power spectrum of the density fluctuations has been normalized so that the r.m.s. mass fluctuation in a sphere of radius $8 h^{-1} Mpc$ takes the value $\sigma_8 = 1$ at the present epoch, $a(t) = a_{fin} = 11$. The simulations are run in an $L = 200 h^{-1} Mpc$ comoving box with $N_p = 84^3$ particles. The gravitational softening parameter of the particles is set to $\varepsilon_g = L/10 N_p^{1/3}$. The filled squares of Fig. 1 show $err(t)$ for a simulation with $\theta = const = 0.4$. This simulation (S1L) was performed using the serial version of the code. With this value of θ one has $err(t) \lesssim 10^{-3}$ even in non-linear regimes, when $a(t)$ approaches its final value. For several values of $a(t)$ the distribution of the relative root mean square errors in the force components of a particle subset ($\sim 5\% N_p$) of the S1L run are displayed in Fig. 2 (left column). The reference forces are calculated from the same particle distribution using $\theta = 0.01$. It has been found that a similar distribution in the relative errors is obtained if during the simulation $\theta = \theta(t)$ increases with time, provided that its value never exceeds an upper limit implicitly defined for $\sigma_8 \geq 0.2$ by the constraint

$$\Delta C/\Delta(aU) \leq 0.025/[1 + (0.4/\sigma_8)^3]^{1.7}. \quad (5)$$

An additional constraint sets an upper limit $\theta \leq 0.9$. A simulation was performed (S2L) with the same input parameters of the run S1L, but with the value of θ now implicitly controlled by Eq. 5. The level of energy conserva-

tion given by the constraint (5) is shown in correspondence of run S2L in Fig. 1 (open squares). The relative errors in the force components of run S2L are plotted in the right column of Fig. 2 for the same particle subset of the run S1L. A more quantitative comparison between the two distributions can be obtained from Fig. 3. The time evolution of the 95% percentile of the cumulative distribution of the relative acceleration errors is plotted for the two runs S1L (open squares) and S2L (filled squares). The relative acceleration error is defined as $\delta a/a \equiv |a - a_D|/|a_D|$, here a_D is the particle acceleration evaluated in the direct summation limit. The results show that for simulation S2L the relative errors in the forces are always below $\sim 3\%$, an upper limit which has been found to yield reasonable accuracy in various tests (Davé, Dubinski & Hernquist 1997, Springel, Yoshida & White 2001, Mocchi & Capuzzo-Dolcetta 2002).

Therefore, the criterion (5) can be profitably used to constrain the value of $\theta(t)$ according to the clustering evolution, and at the same time to maintain the relative errors in the forces below a fixed threshold ($\lesssim 3\%$). This allows a substantial increase in the code performances. The computational cost of evaluating the forces depends on θ and for the considered runs at $a(t) = 11$ it is significantly reduced by a factor of 10 to 20 when θ is increased from 0.4 to ~ 0.9 .

2.4 Multiple timesteps and particle update

After the force calculation is complete, particle velocities and positions are updated in each processor. In the individual timestep scheme (Hernquist & Katz 1989) the particle timestep Δt_i of particle i is determined according to several criteria. The first is important at early epochs and requires that

$$\Delta t_i \leq \Delta t_{exp} = 0.03 \ 2/3 \ H(t), \quad (6)$$

where $H(t)$ is the Hubble parameter at the simulation time t . The other two criteria are

$$\Delta t_i \leq 0.3(\varepsilon_i a^3(t)/g_i)^{1/2} \quad (7)$$

$$\Delta t_i \leq 0.3(\varepsilon_i/v_i), \quad (8)$$

where ε_i is the comoving gravitational softening parameter of the particle i , g_i is the peculiar acceleration and v_i its peculiar velocity. These criteria are similar to those adopted by Davé, Dubinski & Hernquist (1997). Particle timesteps are constrained to take the values $\Delta t_j = \Delta t_o/2^j$, where $j \geq 0$ is an

Table 2
Summary of the simulations

model	N_p ^a	θ ^b	procs ^c	run ^d
Λ CDM	84^3	0.4		<i>S1L</i>
Λ CDM	84^3	var		<i>S2L</i>
CDM	32^3	0.4	P	<i>S3C</i>
CDM	$\sim 35,127$	0.4	P	<i>S4C</i>
CDM	140,608	0.4		<i>S5C</i> (<i>S6C</i> : <i>SPH</i>)

Note ^a : number of particles, for parallel runs is the average number of particles per processor. ^b : the symbol *var* denotes $\theta = \theta(t)$, where θ is implicitly defined according to Eq. 5. ^c procs is the number of processors in the parallel runs. ^d : serial runs are indicated with an *S*, the parallel runs have the same simulation label of the corresponding serial runs but with a subscript added to indicate the processor number *P*. The notation *x* means that the total particle number of the simulation is that of the serial run times the number of processors. The simulation *S6C* is hydrodynamic (SPH), the cosmological and simulation parameters are the same of the run *S5C*, but with a baryonic fraction $\Omega_b = 0.05$. The simulation includes radiative cooling and is performed with $N_p = 140,608$ dark matter and gas particles.

integer. For the particle *i* the timestep Δt_i , which satisfies the above criteria, takes the value Δt_{j_i} such that $\Delta t_{j_i} \leq \Delta t_i$.

At the beginning of the integration $t = t_{in}$, the forces are evaluated for all of the particles and their positions are advanced by half of the initial timestep, which is common to all the particles. In this integration scheme, the forces are evaluated at later times $t > t_{in}$ only for those particles for which it is necessary to maintain the second-order accuracy of the leapfrog integrator. Particles can change their time bins Δt_j and their positions must be corrected to preserve time centering. The transformations necessary to perform these corrections in comoving coordinates are given in appendix A. The particle positions are advanced using the smallest timestep Δt_{min} , as determined by the above constraints. In the parallel implementation, each processor determines the individual particle timesteps and the smallest timestep $\Delta t_{min}^{(pr)}$ of its particle subset, Δt_{min} is then the smallest of these $\Delta t_{min}^{(pr)}$ and is used by all the processors.

After the particle positions have been updated, it may happen that a fraction of the particles assigned to a given processor has escaped the processor subvolume. At each timestep, the particles which are not located within the original processor boundaries are moved between the processors. In principle, the computational cost of locating the processor to which the escaped particle belongs scales as the processor number *P* (Davé, Dubinski & Hernquist 1997, sect. 5.1). However, if during the ORB the processors are partitioned

according to the procedure described in sect. 2.1, the final processor ordering makes it possible to reduce to $\sim \log_2 P$ the number of positional tests of the particle. This is not a significant improvement in pure gravity simulations, where the fraction of particles which leave a processor at each step is small ($\sim 5\%$), but it is important in a future implementation of the code which will incorporate smoothed particle hydrodynamics (SPH; Davé, Dubinski & Hernquist 1997, Springel, Yoshida & White 2001, Springel & Hernquist 2002). In such a scheme, gas properties of a particle are estimated by averaging over a number of neighbors of the particle; in a parallel implementation, an efficient location of the particle neighbors located in the other processors is important in order to improve the code performances.

3 Performances

The treecode described here uses the BH tree algorithm to compute the gravitational forces. The implementation of this algorithm is identical to that of Dubinski (1996) and Davé, Dubinski & Hernquist (1997). The dependence of the errors in the force evaluations on a number of input parameters has been discussed previously by these authors, therefore an error analysis of the forces will not be presented here. It is worth noticing that, in the parallel treecode described here, the tree construction in each processor is such that the gravitational force acting on a particle is identical to that computed by the serial version of the code. For a given particle distribution, a comparison of the values of the forces obtained by the parallel version with the corresponding ones of the serial version can therefore be used to control that there are not bugs in the parallel routines which perform the construction of the local essential trees.

The results of this test are shown in Fig. 4 for a configuration with $P = 8$ processors. The initial positions of $32^3 P$ particles in a $L = 11.11h^{-1}Mpc$ co-moving box have been perturbed according to a CDM model with $\Omega_m = 1$, $h = 0.5$ and power spectrum normalization $\sigma_8 = 0.7$ at the present epoch (simulation *S3C^x_8* of Table 2). This epoch corresponds to a value $a_{fin} = 40$ of the expansion factor and particle forces have been evaluated at $a(t) = 1$. This is because in linear regimes the computation of the forces for a tree code is subject to large relative errors (see sect. 2.3). For a comparison of the forces obtained with different tree codes from the same particle distribution, the choice $a(t) = 1$ then corresponds to the most severe particle configuration to be used with these parameters. Forces have been calculated with an angle parameter $\theta = 0.4$ and quadrupole corrections. To compute parallel forces the particle distribution was split among the P processors. The results plotted in Fig. 4 show that the maximum relative difference between the forces computed by the treecode and its parallel version is $\sim 10^{-8}$. Analogous results were ob-

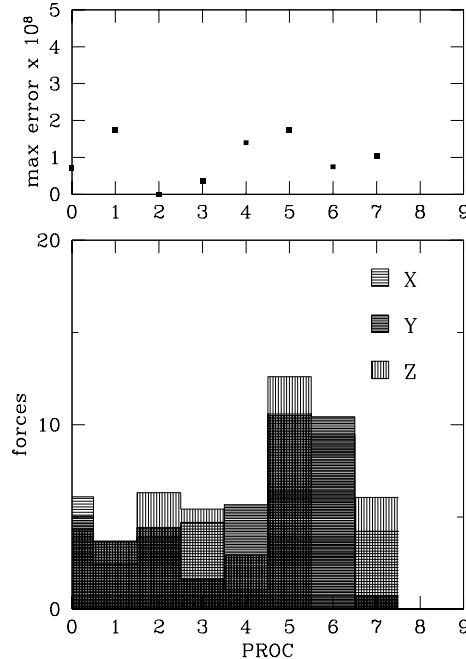


Fig. 4. For the simulation $S3C^x_8$ the upper panel shows the maximum absolute errors in the force components evaluated by each of the $P = 8$ processors at $a(t) = 1$. Reference forces have been calculated with a treecode algorithm applied to the whole distribution of $32^3 P$ particles. The opening angle parameter is $\theta = 0.4$ and cell moments are calculated up to quadrupole order. The bottom panel shows the corresponding values of the forces.

tained for a configuration with $P = 64$ processors. These small differences are presumably due to round-off errors, which lead in the two code versions to differences of the same order in the values of the moments of certain cells. These differences follow because these cells have spatial volumes which occupy two or more processor domains. In the parallel treecode the moments of these cells are then evaluated by summing partial contributions in a different order from that of the serial version. For the simulations of Fig. 1 the values of $\Delta C/\Delta aU$ of the corresponding parallel runs are not shown because they practically overlap with those of the serial runs.

3.1 Scalability

The computational speed of the code is defined as the particle number divided by the elapsed CPU wall-clock time t_{solve} spent in the force computation of the particles. This definition includes also the treewalk necessary for constructing the interaction lists. For a specified accuracy and particle distribution, the CPU time t_{solve} of a parallel treecode with maximum theoretical efficiency is

a fraction $1/P$ of that of the serial code.

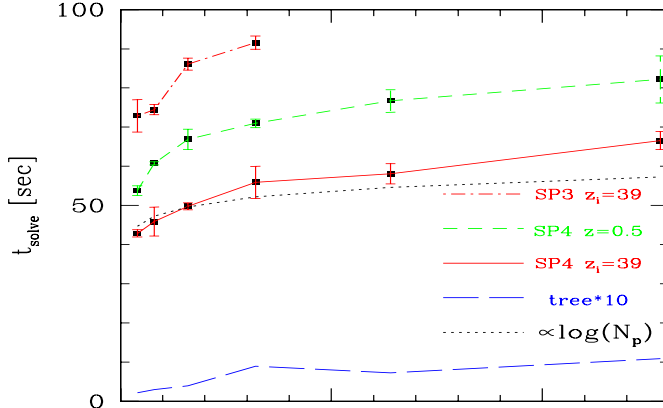


Fig. 5. The average elapsed CPU time t_{solve} spent in the force evaluation as a function of the number of processors P . The value of the opening angle parameter is $\theta = 0.4$, quadrupole moments are taken into account. The error bars are the dispersions over the P processors. The initial particle configuration is found from a uniform distribution perturbed according to a CDM power spectrum at $z_i = 39$. The tests were performed on the IBM SP3 ($P \leq 32$) and SP4 machines ($P \leq 128$). The dash-dot line shows the values of t_{solve} for the tests $S3C^x_P$ on the SP3, continuous line refers to the tests $S4C_P$ on the SP4 (see Table 2). The total particle number of the tests $S4C_P$ is given in Table 3. The short dash line connects the values of t_{solve} obtained from a set of clustered distributions statistically equivalent to that of the runs $S4C_P$ at $z = 0.5$ (see text). The long dashed line is the CPU time for constructing the tree scaled up by a factor 10. The dotted line is the expected t_{solve} from the ideal scaling relation $\propto \log(N_p)$.

The scalability of the parallel treecode was tested by measuring t_{solve} using a different number of processors P . For a configuration of P processors t_{solve} is defined as the average of the values of the individual processors. The tests were performed on the IBM SP3 and SP4 machines hosted by CINECA (Bologna, Italy). In its present configuration the IBM SP4 has 16Gb of RAM memory available on each 8 processor node. The cosmological model is the CDM model previously described. The simulation parameters of the runs, $S3C_P$ and $S4C_P$, are given in Tables 2 & 3. For these runs the number of particles scales linearly with P . This dependence of N_p on P has been chosen in order to compare the force solving CPU time t_{solve} consistently with the one necessary for the construction of the local essential tree. If N_p is kept fixed and P becomes very large the communication time necessary for the

Table 3

Number of particles of the parallel runs $S4C_P$

P^a	N_p	$N_p/P \sim^b$
4	140608	35152
8	287496	35937
16	551368	34460
32	1124864	35152
64	2197000	34328
132	4574296	35737

Note a : number of processors. b : average number of particles per processor.

construction of the local essential trees is expected to be dominant over the force computation and thus code performances will be degraded. On the other hand, this configuration is of scarce practical interest because parallel runs are expected to be performed with a number of particles per processor as high as possible. With the choice $N_p/P = const$, the CPU time t_{solve} scales ideally as $t_{ideal} \propto \log N_p \propto \log P$. The results are shown in Fig. 5, where $t_{solve}(P)$ is plotted up to $P = 128$ (continuous line) for the tests on the SP4 and up to $P = 32$ (dash-dot line) for tests on the SP3. The dotted line shows the ideal scaling relation. In the large P limit t_{solve} is approximately $\sim 10\%$ higher than the ideal scaling relation. This is most probably due to cache effects of the machine which arise when $N_p \gtrsim 10^5$ during the tree descent necessary to calculate the forces. The computational speed at $P = 16$ is $\sim 32^3 P/t_{solve} \sim 400P \text{ part/sec}$ on the IBM SP3, and $\sim 700P \text{ part/sec}$ on the SP4. This is valid for $\theta = 0.4$. If θ is increased, the particle interaction list will have a smaller number of terms and t_{solve} will be smaller. It has been found that $t_{solve}(\theta)$ is well approximated by $t_{solve}(\theta \leq 1) \propto 10^{-5\theta/3}$. If $\theta = 1$ the CPU times of Fig. 5 will then be reduced by a factor ~ 10 .

An important result is the time t_{tree} required to construct the local essential trees. The dashed line of Fig. 5 shows that this time is always a small fraction ($\lesssim 2\%$) of the time required to compute the gravity. It is worth noticing that the communication part is efficiently handled by the all-to-all routine and the corresponding time is a negligible fraction of t_{tree} . This is valid if the accelerations are calculated for the whole particle set. In the parallel implementation of the multistep treecode described here, the local essential trees are constructed at each timestep and the corresponding computational cost is approximately constant, whereas the force solving CPU time t_{solve} depends on the number of active particles at the given timestep. In such cases it may happen that $t_{tree} \geq t_{solve}$. At the end of a large timestep Δt_0 the total tree construction time $t_{tree}(\Delta t_0)$ is defined as the sum of the partial times $t_{tree}(\Delta t_j)$ which have been recorded between $t_n = n\Delta t_0$ and t_{n-1} ; a similar definition holds

also for $t_{solve}(\Delta t_0)$. The ratio $t_{tree}(\Delta t_0)/t_{solve}(\Delta t_0)$ depends on the particle timesteps distribution and the lower limit Δt_{min} . For the tests discussed here $\Delta t_{min} = \Delta t_0/32$ is the minimum considered value of Δt_{min} . According to this constraint it was found that for the considered parallel runs with an evolved clustering state, the ratio $t_{tree}(\Delta t_0)/t_{solve}(\Delta t_0)$ is always small ($\lesssim 10\%$).

In order to assess how $t_{solve}(P)$ scales with P in the strong clustering regime it would be necessary to perform a set of simulations down to $z = 0$ using a different number of processors for the same model. In the large P limit this requires a considerable amount of computational resources. Because the aim of the tests is to obtain an estimate of $t_{solve}(P)$ for a clustered distribution, then $t_{solve}(P)$ can be measured according to the following procedure. A serial run (S5C) was performed using $N_p = 140,608$ particles, with the same cosmological parameters and initial conditions of the tests $S4C_P$. The run was evolved from $z_i = 39$ to $z = 0$. The maximum timestep takes the value $\Delta t_0 = t_{fin}/424$, and $\Delta t_{min} = \Delta t_0/32$. Particles timesteps are constrained according to Eqs. 6,7 and 8. The redshift $z = 0.5$ corresponds to a simulation time $t_n = n\Delta t_0 = 228\Delta t_0$. At this redshift the particle distribution was divided within the computational volume L^3 using the ORB procedure and particle computational weights calculated at the previous step. The four subvolumes and their corresponding particle distributions were given as initial conditions to the parallel treecode with $P = 4$ processors. The average number of particle per processor is $\sim 35,000$ and is that of $S4C_P$. The first point of the CPU time $t_{solve}(P)$ at $z = 0.5$ is then measured as in the previous test at $z_i = 39$. For a larger number of processors (up to $P = 32$), clustered distributions statistically equivalent to those of the tests $S4C_P$ can be obtained as follows. The four subvolumes of the test with $P = 4$ processors and $N_p(P)$ particles have lower bottom corners with coordinates xb_p^m , sizes l_p^m and volumes $V_p = l_p^1 l_p^2 l_p^3$, where p is the processor index and m is the axis index. The subvolumes are divided along a cartesian axis m_1 into two new separate equal volumes $V_p/2$, the particles which belong to the original subvolumes have now half the original mass and coordinates $x_i^{m_1} \rightarrow xb_p^{m_1} + (x_i^{m_1} - xb_p^{m_1})/2 = x_i^{m_1}(1)$. In each of the original subvolumes the particle distribution is then replicated creating a new set of $N_p(P)$ particles with coordinates $x_i^{m_1}(2)$ given by $x_i^{m_1}(2) = x_i^{m_1}(1) + l_p^{m_1}/2$ and all of the other variables left unchanged. This procedure can then be repeated along the other two axes to generate up to 8 subdivisions from each of the four subvolumes used for the test with $P = 4$. To measure $t_{solve}(P)$ at $z = 0.5$ for $P = 64(P = 128)$ this splitting procedure is first applied along one (two) cartesian axis to the whole particle distribution within the computational volume L^3 . The new distributions are divided among 8 (16) subvolumes and the procedure described above is used to generate for each of the subvolumes 8 new subdivisions. After the whole procedure has been completed, the final particle distributions within the original volume L^3 are then used as initial conditions for measuring $t_{solve}(P)$ using the parallel treecode with $P = 64$ or $P = 128$. The obtained values of $t_{solve}(P)$ range

from $P = 4$ up to $P = 128$ and are displayed in Fig. 5 (short-dash line). These values are supposed to give a fair estimate of what would be those obtained running the tests $S4C_P$ down to $z = 0.5$. The results show that $t_{solve}(P, z = 0.5)$ scales with P as $t_{solve}(P, z_i = 39)$ in the linear regime; this demonstrates that the overall scalability of the code does not depend upon the degree of clustering of the particle distribution.

A comparison of the code performances with those of other authors is difficult because of different algorithms, particle distributions and machines. The plots of Fig. 5 show that the values of t_{solve} on the IBM SP4 are only a factor ~ 2 smaller than the corresponding ones measured on the IBM SP3, though the SP4 has a clock-rate which is ~ 3.5 ($1.3GHz$) faster than that of the SP3 ($375MHz$). These relatively poor code performances on the SP4 must be attributed to the different hardware architectures and size of the memory caches in the two machines, see Genty et al. (2002) for the relative documentation on the SP4. In order to compare code performances with those illustrated in other papers it is more appropriate to refer to the values of t_{solve} measured with the IBM SP3. An educated guess that the code has performances fairly comparable with those of the Springel, Yoshida & White (2001) code is given by Fig. 12 of their paper. In this figure the gravity speed as a function of the processor number is shown for a cosmological hydrodynamic SPH simulation in a comoving box size of $50h^{-1}Mpc$ with 32^3 dark matter particles and 32^3 gas particles. The cosmology is given by a Λ CDM model with $\Omega_m = 0.3$ and $h = 0.7$. The simulations were evolved from an initial redshift $z_i = 10$. The plotted speeds were measured on a CRAY T3E ($300MHz$ clock). From Fig. 12 the computational speed of gravity for $P = 32$ is $\sim 7500part/sec$. The cosmological model is not that adopted in the tests of Fig. 5, but at early redshifts the computational cost of the gravity force calculation is not strongly dependent on the assumed model. For $P = 32$ and $\theta = 0.4$ the results of Fig. 5 give a gravity speed of $\sim 12 \cdot 10^3part/sec$ on the IBM SP3 for a CDM model at $z_i = 39$. The measured speed must be reduced by $\sim 20\%$ to take into account the higher clock-rate of the IBM SP3 ($375MHz$). The final value ($\sim 9500part/sec$) is similar to the one obtained by Springel, Yoshida & White (2001). It must be stressed that the timings shown in Fig. 5 are the worst case to be considered for a comparison with the gravity speeds reported in Fig. 12 of Springel et al. (2001). This is because the clustering evolution is expected to allow a decreasing value of $\theta(t)$ and thus a corresponding increase in the computational speed. The CPU times t_{solve} of Fig. 5 refer to the gravitational force calculation with $\theta = 0.4$ of a particle distribution at high redshifts, whereas the speeds in Fig. 12 of Springel, Yoshida & White (2001) are defined over the entire range of the simulation time. The particle forces of the tests shown in Fig. 5 were evaluated applying the improved BH criterion (2) with $\theta = 0.4$ and quadrupole moments to the particle distributions. For $P = 4$ the corresponding particle interaction lists have at $z_i = 39$ a mean number of terms $\langle w \rangle \sim 1,000$. The distribution of the relative acceleration

errors shows that 95% of the particles have $\delta a/a \lesssim 10^{-2}$. These results can be compared with those displayed in Fig. 7 of Springel, Yoshida & White (2001), where the 95% percentile of the cumulative distribution of the relative force errors $\delta a/a (< 95\%)$ is plotted versus $\langle w \rangle$ in a 32^3 cosmological simulation at $z_i = 25$. The plots are for different opening criteria. At $\theta = 0.4$ the new opening criterion of Springel, Yoshida & White (2001) gives a comparable accuracy with approximately the same number of terms.

Another comparison can be made with the parallel treecode developed by Micchi & Capuzzo-Dolcetta (2002). The authors computed gravity speeds on a CRAY T3E for a Plummer distribution with $N_p = 128,000$ particles. Fig. 7 of their paper shows $\delta a/a (< 90\%)$ versus the average work $\langle w \rangle$ per particle. The forces were calculated using the BH criterion with quadrupole moments. The maximum value of $\langle w \rangle$ in the figure is $\sim 1,000$, and it corresponds to $\delta a/a (< 90\%) \sim 10^{-3}$. For a configuration of $P = 32$ processors this value of $\delta a/a (< 90\%)$ gives a gravity speed of about $\sim 10^4 \text{part/sec}$ (Fig. 5 of their paper). Taking into account the different clock rates of the machines used in the tests, this value of the speed is approximately that obtained here on the IBM SP3 with the same number of processors and an interaction list of nearly equal length. Finally, it is worth noticing that the ratio t_{tree}/t_{solve} is significantly lower than that obtained in other parallel versions of a treecode (Dubinski 1996, Springel, Yoshida & White 2001).

3.2 Load balancing

An important characteristic of a treecode is load balancing. An ideal code should have the computational work divided evenly between the processors. This is not always possible and code performances will be degraded when the load imbalance between the processors becomes large. At any point of the code where synchronous communications are necessary there will be $P-1$ processors waiting for the most heavily loaded one to complete its computational work. Load balancing can then be measured as

$$L = \frac{1}{P} \sum_p 1 - (t_{max} - t_p)/t_{max}, \quad (9)$$

where t_p is the CPU time spent by the processor p to complete a procedure and t_{max} is the maximum of the times t_p . A treecode spends most of the CPU time in computing gravitational forces, and so it is essential to have good load balancing ($\gtrsim 90\%$) with the gravity routine. As already outlined in sect. 2.1 this task is not obviously achieved with a multistep treecode. The number of active particles N_{act} between the simulation times t_n and $t_n + \Delta t_0$ can vary wildly as a function of the current simulation time $t_n^{(k)}$. This is defined k steps

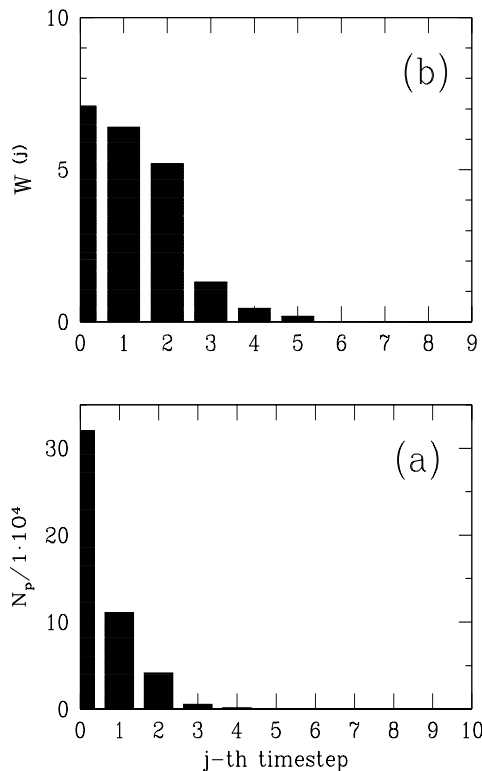


Fig. 6. **(a)**: Number of particles with timesteps $\Delta t_j = \Delta t_0/2^j$ at the end of a macrostep Δt_0 for the serial run S6C. The number of particles is 479,445, $\Delta t_0 = t_{fin}/424$, $\Delta t_{min} = \Delta t_0/32$ and simulation time $t_n = n\Delta t_0 = 228\Delta t_0$. The simulation is hydrodynamic according to the SPH method, and includes radiative cooling and star formation. The number of particles includes also the star particles which have been formed since the initial simulation time. **(b)**: For the same particle distribution the corresponding computational loads $W^{(j)} = \sum_{i \in \Delta t_j} W_i$ are shown. The summation is over all the particles i with timesteps Δt_j .

after t_n as $t_n^{(k)} = t_n + \sum_{j=1}^{j=k} \Delta t_j$, the summation is at $t > t_n$ over the past timesteps Δt_j .

At a certain step the ORB procedure described in sect. 2.1 can be used to obtain load balancing, but at later steps the unbalancing can be substantial. This problem has prompted some authors to consider more complicated approaches (Springel, Yoshida & White 2001, Mocchi & Capuzzo-Dolcetta 2002). Here a simpler route is followed starting from the observation that in a multistep integration scheme, a better measure of the computational work done by each particle i is given by $W_i = \sum_k w_i^{(k)}$, where $w_i^{(k)} \propto N_{OP}(i)$ is the number of floating point operations of particle i necessary to calculate the gravitational forces of the particle at the simulation time $t_n^{(k)}$. If the particle i is not active at $t_n^{(k)}$, $w_i^{(k)} = 0$. The summation is over the steps between t_n and $t_n + \Delta t_0$, the weights W_i are now used at each large step Δt_0 to subdivide the computational volume according to the ORB procedure. Theoretically, this weighting scheme does not guarantee a perfect load balance, nonetheless it has been found to yield satisfactory results ($L \gtrsim 90\%$) in many typical applications. The reason lies in the shape of the distribution function $F(\Delta t_i)$ of the particle timesteps

Δt_i , for a simulation with an evolved clustering state. The number of particles with timesteps in the interval $\Delta t_j, \Delta t_j + \Delta t$ is given by $n_j = F \Delta t$. The particle timesteps are determined according to the criteria defined in sect. 2.4. Another parameter which determines the shape of the distribution function is the minimum timestep Δt_{min} . The optimal choice for Δt_{min} requires that the number of particles of the binned distribution n_j in the last time bin should be a small fraction of the total particle number, as a rule of thumb it is found $N_{opt} \sim 5\% N_p$. The particles in the last time bin are n_{jmax} with timesteps $\Delta t_{min} = \Delta t_{jmax} = \Delta t_0 / 2^{jmax}$. If n_{jmax} is much higher than the threshold N_{opt} it means that the integration scheme is not accurate, for a specified set of constraints on the particle timesteps, because there are many simulation particles with $\Delta t = \Delta t_{min}$. On the other hand, if $n_0 \sim N_p$, it would imply that the computational work of the code is wasted for the required accuracy.

The binned distribution n_j was measured for a clustered particle distribution originated from a serial (S6C) test simulation. This simulation is similar to the serial run S5C of sect. 3.1, but incorporates now hydrodynamics according to the SPH scheme. The cosmological parameters are the same as S5C, but with a baryonic density parameter $\Omega_b = 0.05$. These values are the same simulation parameters used by Davé, Dubinski & Hernquist (1997, sect. 4.3) for testing their parallel SPH treecode. The run was performed from $z_i = 39$ down to $z = 0$ using an equal number of 140,768 gas and dark matter particles. The simulation includes radiative cooling, an ionizing UV background and gas particles in cold high density regions are subject to star formation. For more details see, e.g., Valdarnini (2002b). The maximum timestep takes the value $\Delta t_o = t_{fin}/424$, and $\Delta t_{min} = \Delta t_0/32$ is the minimum allowed timestep of dark matter particles according to the criteria defined in sect. 2.3; gas particles have their timesteps additionally constrained by the Courant condition (Hernquist & Katz 1989). At the simulation time $t_n = n \Delta t_0 = 228 \Delta t_0$, the particle distribution of the simulation was used, following the splitting procedure described in sect. 3.1, for generating the initial conditions for the parallel simulations. The parallel runs are purely collisionless and gas particles were treated as dark matter particles. These simulations were performed to investigate the load balancing efficiency of the parallel treecode. According to the previous discussion, the load balancing parameter L depends on the shape of the distribution function of the particle timesteps. For this reason it was decided to generate initial conditions for the parallel runs from an SPH simulation. Hence, the measured performances are indicative of those that would be obtained if SPH were to be implemented in the parallel code.

The distribution n_j of the simulation S6C is shown as a function of the particle timesteps Δt_j in Fig. 6a, at the simulation time $t_n = n \Delta t_0 = 228 \Delta t_0$. The corresponding distribution of particle computational loads W_i is shown in panel (b). The plotted distribution is $W^{(j)} = \sum_{i \in \Delta t_j} W_i$, the summation being over all of the particles i with timesteps Δt_j . About $\sim 90\%$ of the particles are

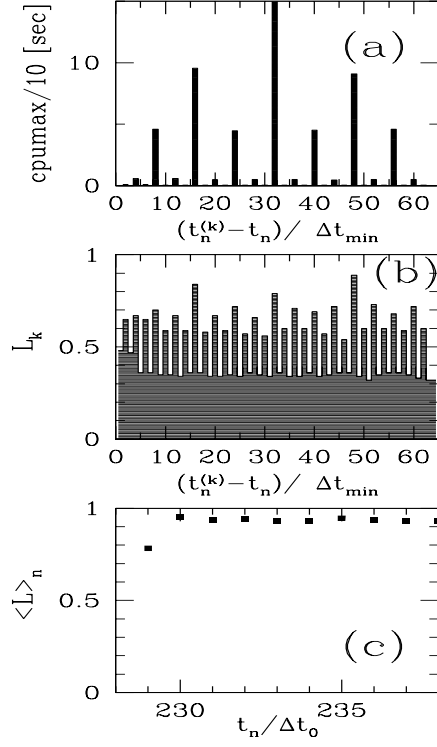


Fig. 7. The load balancing scheme is tested for a parallel run with $P = 4$ processors. The initial conditions have been obtained from the clustered particle distribution of simulation S6C (see Fig. 6). **(a)**: The top panel shows, between t_n and t_{n+1} , the maximum of the CPU times of the P processors at the simulation time $t_n^{(k)}$, $n = 228$. The corresponding load balancing L_k is plotted in the mid panel **(b)**. The bottom panel shows the load balancing $\langle L \rangle_n$ at the end of each macrostep Δt_0 . The validity of the weighting scheme is shown by the first point, where the ORB procedure has been performed setting $w_i = \text{const}$.

in the first three time bins. It can be seen that for these bins the variations in the load distribution are within $\sim 20\%$. For example, the number of particles n_j with timestep $\Delta t_3 = \Delta t_0/8$ is $\sim n_0/10$. The choice of a simple weighting scheme $w_i \propto N_{OP}(i)$ would have given a shape of the load distribution similar to that of n_j . The reason for the shape of the load distribution of Fig. 6b is that in a multistep integration scheme the particle forces are calculated within a large timestep Δt_0 when their positions must be synchronized. An optimal choice of the constraints on the particle timesteps yields a binned distribution n_j with a hierarchy $n_{j+1} \sim n_j/2$. A weighting scheme which sums the number of floating point operations over a large timestep Δt_0 takes into account the

fact there are few particles with $\Delta t_j \ll \Delta t_0$ but that these particles have forces calculated a number of times $\propto \Delta t_j^{-1}$. This weighting scheme leads, at the end of a large timestep Δt_0 , to particle loads with a distribution which can be considered roughly constant, for practical purposes, for a large fraction of the simulation particles ($\sim 90\%$). An ORB domain decomposition is then applied every large timestep Δt_0 according to the calculated weights of the particles. The subdivision of the computational load that follows from this ORB among the processors is still unbalanced, but within a large timestep Δt_0 the unbalancing is higher when the computational work is minimal.

Finally, the load balancing efficiency of the proposed weighting scheme was tested against the processor number P by measuring $\langle L \rangle_n$ for a set of runs. The binned distribution n_j of Fig. 6 reveals that there are few particles with timesteps $\Delta t_j = \Delta t_5$, the parallel runs were performed setting $\Delta t_{min} = \Delta t_0/32$. The initial conditions for the runs with $P \leq 128$ processors were obtained from simulation S6C as previously discussed. For $P = 4$ the relative weights of the different computational works within a large timestep Δt_0 are clearly illustrated in Fig. 7. Panel (a) shows the elapsed CPU wall-clock time spent by the parallel code to compute the gravitational forces. The CPU time is plotted between t_n and t_{n+1} versus the simulation time $t_n^{(k)}$ and is the maximum of the single processor values. There is a large burst of CPU work when the particles synchronized at $t_n^{(k)}$ are those with timesteps Δt_0 , $\Delta t_0/2$ and $\Delta t_0/4$. The instantaneous load balancing $L_{(k)}$ is shown in panel (b) and is calculated using Eq. 9 between $t_n^{(k)}$ and $t_n^{(k+1)}$. The CPU times t_p refer to the times spent in the gravity force computation but without including those necessary for the construction of the local trees. It can be seen that $L_{(k)}$ drops to very inefficient values ($\lesssim 0.3$) when $t_n^{(k)}$ corresponds to a small number of active particles and it reaches a high efficiency ($\gtrsim 0.9$) with the highest CPU times. The overall load balancing is measured by applying Eq. 9 between every ORB domain decomposition; panel (c) shows $\langle L \rangle_n$ versus the simulation time t_n for ten large timesteps Δt_0 . The ORB procedure was performed setting for the first step $w_i = const$, yielding $\langle L \rangle_n \sim 0.8$. This proves that the load balancing performances are sensitive to the chosen weighting scheme and that the procedure previously described is optimal to achieve a good load balance for the parallel treecode described here.

In Fig. 8 the values of $\langle L \rangle_n$ for the parallel runs are displayed versus the processor number P . For each value of P , the values of $\langle L \rangle_n$ were computed for three timesteps Δt_0 . The CPU times used for computing $\langle L \rangle_n$ include also the tree construction times. The measured values of $\langle L \rangle_n$ demonstrate that this weighting scheme for the ORB domain decomposition can be successfully used to obtain an efficient load balancing, even when the number of processors is high. These performances are not affected if the measured CPU times used for computing $\langle L \rangle_n$ do not include the tree construction parallel overheads. For $P=32$ it is found $t_{tree}(\Delta t_0)/t_{solve}(\Delta t_0) \sim 5\%$ and for $P = 128$

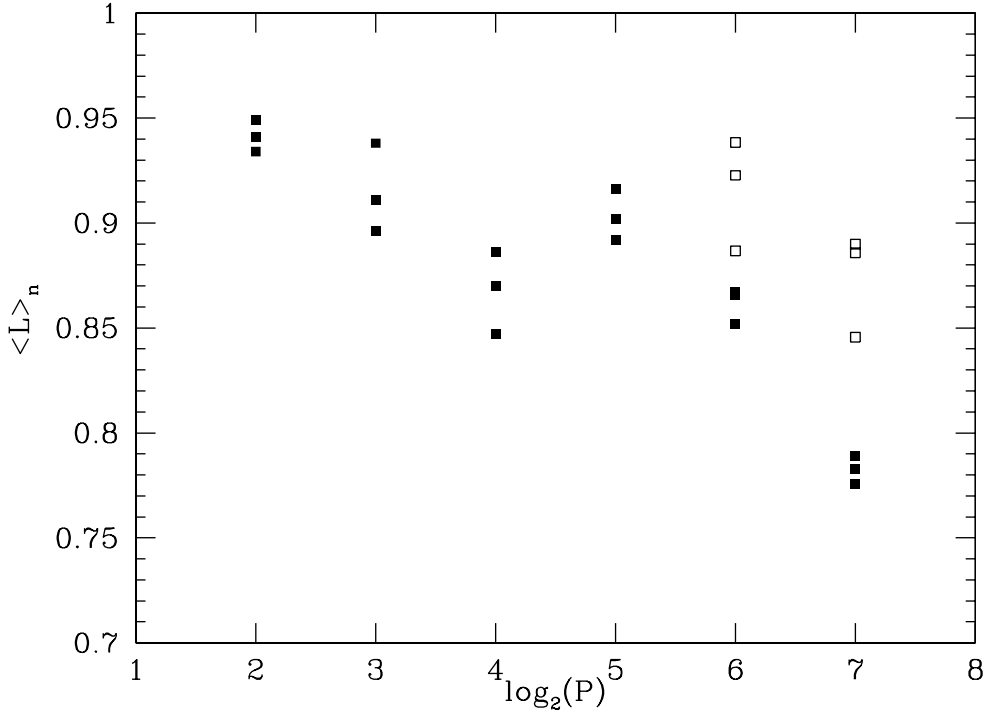


Fig. 8. For a set of parallel runs the values of the load balancing $\langle L \rangle_n$ at the end of a timestep Δt_0 are shown for three timesteps versus the processor number P . Initial conditions were obtained from the serial run *S6C* (Fig. 6), using the splitting procedure described in sect. 3.1. For $P \geq 64$ open symbols refer to the values of $\langle L \rangle_n$ evaluated according to the computational loads used to perform the ORB subdivision.

this ratio grows up to $\sim 10\%$. This is an important feature of the parallel treecode presented here, since in a multistep treecode the tree reconstruction at each timestep can degrade code performance. Parallel runs with $P = 128$ have load balancing down to $L \sim 0.8$. It must be stressed that, for $P > 32$, these relatively poor values of the load balancing are not due to a failure of the adopted weighting procedure. About a $\sim 10\%$ of the loss of balancing efficiency originates from the scatter of the CPU times among different processors with the same amount of computational load. This is clearly illustrated by the open symbols of Fig. 8. For $P \geq 64$ these symbols refer to the values of $\langle L \rangle_n$ evaluated at the end of the step $t_n = n\Delta t_0$ using in Eq. 9 the computational loads of each processor p : $W_p \equiv \sum_i W_i$, instead of the corresponding CPU times. The particle computational loads W_i are those used to perform the ORB procedure, hence the load balancing measured according to the processor values W_p yields a sort of ‘theoretical maximum’ balancing efficiency for the chosen weighting scheme. Fig. 8 shows that for $P \geq 64$ the values of $\langle L \rangle_n$ measured using the computational loads are systematically higher (~ 0.9) than those obtained from the CPU times of the processors. For $P = 128$, the processor computational loads versus the corresponding CPU times t_p are presented in Fig. 9 at the simulation time $t_n^{(k)} = 228\Delta t_0 + \Delta t_0/2$. The large scatter among the values of t_p for a given computational load shows that the relatively poor code performances in the large P regime are not then intrinsic to the proposed weighting method for performing the ORB parti-

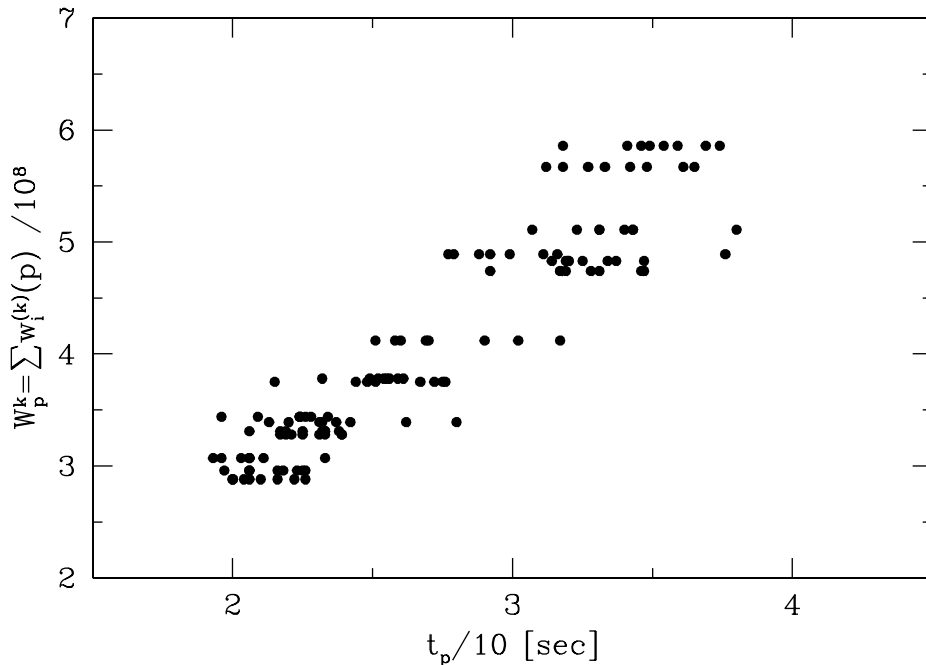


Fig. 9. For the parallel run of Fig. 8 with $P = 128$ the computational loads W_p^k of the processors are plotted at the simulation time $t_n^{(k)}$ versus the corresponding CPU times t_p , here p is the processor index. W_p^k is defined as the sum over the processor particles of the loads $w_i^{(k)}$. The particle computational loads $W_i = \sum_k w_i^{(k)}$ are those used to perform the ORB procedure. The simulation time is chosen at $t_n^{(k)} = 228\Delta t_0 + \Delta t_0/2$, when there is the highest number of active particles.

tion, but arise because of the scattering of the CPU times between processors with the same computational load, which increases as P increases. The scatter of the CPU times is attributable to the probability of having the memory access of a process in conflict with concurrent tasks. This probability grows statistically as P increases and it depends on the machine configuration.

The above runs have illustrated the load balancing efficiency L ($\sim 90\%$) for a set of simulations with an evolved clustering state, but at high redshifts the values of L for a cosmological simulation are equally high. This follows because in a multistep integration scheme the particles have initially assigned the smallest timestep Δt_{min} . The main criterion which determines particle timesteps at early redshifts is given by Eq. 6. There is thus a large fraction of particles which, during the early phases of the simulation, evolves with the same timestep. For a ‘monochromatic’ distribution function of particle timesteps, the load balancing that follows from the ORB procedure is similar to the one of the single-step integration scheme and is as high as that of a clustered distribution. This confirms that the load balancing efficiency of the adopted weighting scheme is robust for a variety of clustering states in cosmological simulations.

The high load balancing efficiency of the code compares well with the values reported for the gravity computation by Davé, Dubinski & Hernquist (1997) in several tests on the performances of their parallel treecode which incorporate SPH hydrodynamics. For a number of processors $P \leq 16$ the obtained values

of L are higher than those presented by Springel, Yoshida & White (2001, Table 1), and similar to the ones of Miocchi & Capuzzo-Dolcetta (2002, Fig.6). A proper comparison is difficult however, because the tests of these authors were performed keeping the number of particles constant, while increasing the processor number. The implementation of SPH hydrodynamics in the parallel treecode is a work in progress, however it is unlikely that the performances of the parallel treecode combined with SPH will be degraded. According to the tests performed by Davé, Dubinski & Hernquist (1997, Table 1), for $P = 8$ processors the SPH computational part of the code is load balanced to $\sim 97\%$. For the gravity computation, the value is similar and in the same range as those found here with the same number of processors.

4 Summary and conclusions

A parallel treecode which is designed for running cosmological N -body simulations on parallel machines with distributed memory has been discussed. The code uses individual timesteps and the gravitational field is solved according to the BH algorithm. In this method the accuracy of the individual particle accelerations is controlled by the value of the opening angle parameter θ . The code uses a value of $\theta = \theta(t)$ which varies with the simulation time t during the integration. The optimal value is chosen to minimize the computational work for evaluating the particle accelerations while keeping the relative errors below a fixed threshold. The domain decomposition of the computational volume among the processors is performed according to the ORB procedure using a suitable chosen weighting scheme to measure the particle computational loads. To compute the gravitational accelerations of the local particles of each processor it is necessary to construct first the local essential trees. The construction of the local essential trees follows that already implemented in previous works (Dubinski 1996, Davé, Dubinski & Hernquist 1997). In sect. 2.3 it was seen that it is possible to concentrate all the communications between processors, necessary for the construction of the local essential trees, in a single phase, which can be efficiently managed with a single message-passing all-to-all routine.

The parallel performances of the code were tested on two different machines (IBM SP3 and SP4) and for a set of parallel runs up to $P = 128$ processors. For a fixed value of θ and keeping constant the number of particles per processor, it is found that the CPU time t_{solve} required to compute the gravitational accelerations is well approximated by the expected theoretical scaling relations $\propto \log(N_p)$, with a $\sim 10\%$ loss in the large $P(\geq 64)$ limit. The results show that the computational cost t_{tree} necessary for the construction of the local trees is a small fraction of the time t_{solve} . This is important because according to the parallel scheme presented here the trees must be

reconstructed in the processors domains at each timestep. This could degrade code performance in a multistep scheme where the number of active particles and then the gravity computational work of the code strongly depend on the current timestep. An important issue related to this point is the load balancing efficiency of the code when individual timesteps are used. In a multistep integration scheme, the work load imbalance among the processors can be significant at each timestep. The measured performances show that this task can be efficiently solved if the domain decomposition of the computational volume among the processors is done using an appropriate weighting of the computational work carried out on each particle within a large timestep. The results of the parallel runs show that the load balancing is very weakly dependent on the particle clustering distribution, and is as high as $\sim 90\%$ up to $P = 32$. When a larger number of processors is used, code performances are degraded down to $\sim 80\%$. This relatively low efficiency in the large P limit follows because, for a given computational load, the scatter between the processor CPU times increases as P increases. If the load balancing is measured according to the computational load of the processor particles, it is found that $L \sim 90\%$ up to $P = 128$. This shows that the intrinsic efficiency of the proposed load balancing algorithm is as high as $\sim 90\%$ and this is the expected value that can be obtained in the large P regime on a memory dedicated machine.

To summarize, it has been shown that a multistep parallel treecode can be used to run cosmological simulations on massive parallel machines with low communication overheads ($\lesssim 5\%$), a speedup $\sim 10\%$ lower than its theoretical value and a good load balancing ($\sim 90\%$ up to $P = 32$). The performances of the proposed algorithms for the parallelization of a treecode should then be considered particularly promising. This is because the continuous growth of computer technology is likely to make cosmological simulations on parallel machines with a very large array of processors routinely available in forthcoming years.

5 Acknowledgements

The author is grateful to C. Cavazzoni, of the CINECA staff, for helpful comments and discussions on parallel algorithms and the implementation of the code.

Appendix A: Time integration in comoving coordinates

The equation of motions of the particles are defined in comoving coordinates as follows:

$$\begin{aligned}\frac{d\vec{x}}{dt} &= \vec{v}, \\ \frac{d\vec{v}}{dt} &= \frac{\vec{g}}{a(t)^3} - 2H(t)\vec{v},\end{aligned}\tag{A-1}$$

where $\vec{r} = a(t)\vec{x}$ is the proper distance, $a(t)\vec{v}$ is the peculiar velocity and \vec{g}/a^2 is the peculiar acceleration. It is useful to introduce the notation $\vec{g}' \equiv \vec{g}/a^3$. The particle positions and velocities are advanced according to a second order leapfrog integrator. The spatial coordinates at the step $n + 1/2$ and the velocities at the step $n + 1$ are then, respectively, given by

$$\begin{aligned}\vec{x}_{n+1/2} &= \vec{x}_{n-1/2} + \Delta t \vec{v}_n, \\ \vec{v}_{n+1} &= \vec{v}_n + \Delta t [\vec{g}' - 2H\vec{v}]_{n+1/2} = \\ &= \vec{v}_n \left[\frac{1-\Delta t H}{1+\Delta t H} \right]_{n+1/2} + \Delta t \left[\frac{\vec{g}'}{1+\Delta t H} \right]_{n+1/2},\end{aligned}\tag{A-2}$$

where the variables in square brackets are evaluated at the timestep indicated by the subscript and $\vec{v}_{n+1/2} = (\vec{v}_{n+1} - \vec{v}_n)/2$. At the beginning of the integration all of the particles have the same timestep $\Delta t = \Delta t_{min}$, and the particle positions are centered at half time step according to

$$\vec{x}_{n+1/2} = \vec{x}_n + \frac{\Delta t}{2} \vec{v}_n + \frac{\Delta t^2}{8} [\vec{g}' - 2H\vec{v}]_n.\tag{A-3}$$

If it is necessary to synchronize at the step $n + 1$ the particle positions with the velocities, then \vec{x}_{n+1} is given by

$$\begin{aligned}\vec{x}_{n+1} &= \vec{x}_{n+1/2} + \frac{\Delta t}{2} \vec{v}_{n+1/2} + \frac{\Delta t^2}{8} [\vec{g}' - 2H\vec{v}]_{n+1/2} = \\ &= \vec{x}_{n+1/2} + \frac{\Delta t}{2} \vec{v}_{n+1} + \frac{\Delta t^2}{4} \vec{v}_{n+1} \left[\frac{H}{1-H\Delta t} \right]_{n+1/2} \\ &\quad - \frac{\Delta t^2}{8} \left[\vec{g}' \frac{1+H\Delta t}{1-H\Delta t} \right]_{n+1/2},\end{aligned}\tag{A-4}$$

where the mid-point velocity $\vec{v}_{n+1/2}$ is estimated using

$$\vec{v}_{n+1} = \vec{v}_{n+1/2} + \frac{\Delta t}{2} [\vec{g}' - 2H\vec{v}]_{n+1/2}.\tag{A-5}$$

When a particle changes its timestep from Δt_{old} to Δt_{new} , its position must be corrected in order to preserve second order accuracy. The correction terms are

$$\vec{x} \rightarrow \vec{x} + \left(\frac{\Delta t_{new}^2}{8} - \frac{\Delta t_{old}^2}{8} \right) [\vec{g}' - 2H\vec{v}]_{n+1/2}, \quad (\text{A-6})$$

the subscript of the term in square brackets refers to the last time the acceleration of the particle has been evaluated. Using Eq. A.5 this term can be written as

$$[\vec{g}' - 2H\vec{v}]_{n+1/2} = \left[\frac{\vec{g}'}{1 - H\Delta t} \right]_{n+1/2} - \left[\frac{2H}{1 - H\Delta t} \right]_{n+1/2} \vec{v}_{n+1}. \quad (\text{A-7})$$

References

- Appel, A.W. 1985, SIAM, J. Sci. Stat. Comp, 6, 85
- Barnes, J.E. 1990, JCP, 87, 161
- Barnes, J.E. 1994, In Computational Astrophysics, Eds. J. Barnes et al., Springer-Verlag
- Barnes, J. & Hut, P. 1986, Nature, 324, 446
- Bertschinger, E. 1998, ARA&A, 36, 599
- Davé, R., Dubinski, J. & Hernquist, L. 1997, NewA , 2, 277
- Dubinski, J. 1996, NewA, 1, 133
- Genty, M., Ha, S.-K., Pirraglia, T., Quintero, D., Radu, G. & Ramos, M. 2002, ‘Performances and tuning considerations for the p690 in a cluster 1600’, IBM Red Book manual , at <http://www.ibm.com/redbook>
- Hernquist, L. 1987, ApJS, 64, 715
- Hernquist, L. & Katz, N. 1989, ApJS, 70, 419
- Hernquist, L., Bouchet, F.R. & Suto, Y. 1991, ApJS, 75, 231
- Lia, C. & Carraro, G. 2000, MNRAS, 314, 145
- Miocchi, P. & Capuzzo-Dolcetta, R. 2002, AA, 382, 758
- Salmon, J. 1991, Ph.D. Thesis, California Institute of Technology
- Springel, V., Yoshida, N. & White, S.D.M. 2001, NewA, 6, 79
- Springel, V. & Hernquist, L. 2002, 333, 649

Valdarnini, R. 2002a, in "Computational astrophysics in Italy: methods and tools",
Bologna july 4-5 2002, ed. R. Capuzzo- Dolcetta, Mem. SAIIt, Suppl., in press

Valdarnini, R. 2002b, ApJ, 567, 741

Warren, M.S. 1994, Ph.D Thesis, University of California, Santa Barbara